

Sub-Doppler Frequency Metrology in HD for Tests of Fundamental Physics

F. M. J. Cozijn,¹ P. Dupré,² E. J. Salumbides,¹ K. S. E. Eikema,¹ and W. Ubachs¹

¹*Department of Physics and Astronomy, LaserLaB, Vrije Universiteit Amsterdam, de Boelelaan 1081, 1081 HV Amsterdam, The Netherlands*

²*Laboratoire de Physico-Chimie de l'Atmosphère, Université du Littoral Côte d'Opale, 189A Avenue Maurice Schumann, 59140 Dunkerque, France*



(Received 22 December 2017; published 9 April 2018)

Weak transitions in the (2,0) overtone band of the hydrogen deuteride molecule at $\lambda = 1.38 \mu\text{m}$ were measured in saturated absorption using the technique of noise-immune cavity-enhanced optical heterodyne molecular spectroscopy. Narrow Doppler-free lines were interrogated with a spectroscopy laser locked to a frequency comb laser referenced to an atomic clock to yield transition frequencies [$R(1) = 217105181895(20)$ kHz; $R(2) = 219042856621(28)$ kHz; $R(3) = 220704304951(28)$ kHz] at three orders of magnitude improved accuracy. These benchmark values provide a test of QED in the smallest neutral molecule, and they open up an avenue to resolve the proton radius puzzle, as well as constrain putative fifth forces and extra dimensions.

DOI: [10.1103/PhysRevLett.120.153002](https://doi.org/10.1103/PhysRevLett.120.153002)

Molecular hydrogen, the smallest neutral molecule, has evolved into a benchmark quantum test system for fundamental physics now that highly accurate measurements challenge the most accurate theoretical calculations, including relativity and quantum electrodynamics (QED) [1,2], even to high orders in the fine structure constant (up to $m\alpha^6$) [3]. The measurement of the H_2 dissociation energy [4] was a step in a history of mutually stimulating advancement, in both theory and experiment, witnessing an improvement over seven orders of magnitude since the advent of quantum mechanics [5]. Accurate results on the fundamental vibrational splitting in hydrogen isotopologues [6], with an excellent agreement between experiment and theory, have been exploited to put constraints on the strengths of putative fifth forces in nature [7] and on the compactification of extra dimensions [8].

A straightforward strategy to obtain accurate rovibrational level splittings in the hydrogen molecule is to measure weak quadrupole transitions, as was done for H_2 in the first [9] and second overtone band [10,11], as well as in the fundamental [12] and overtone [13,14] bands of D_2 . In the heteronuclear isotopologue hydrogen deuteride (HD), exhibiting a charge asymmetry and a weak dipole moment [15], a somewhat more intense electric dipole spectrum occurs, first measured by Herzberg [16]. The dipole moment of the (2,0) band is calculated at $20 \mu\text{D}$ [17], in reasonable agreement with experiment [18,19]. Accurate Doppler-broadened spectral lines in the HD (2,0) band were reported using sensitive cavity ring down techniques [19]. These lines exhibit a width in excess of 1 GHz at room temperature, which challenges the determination of center frequencies in view of various speed-dependent collisional broadening and shifting phenomena

[20]. Careful line shape analysis has led to accuracies of ~ 30 MHz, in accordance with the *ab initio* calculated values [21].

Here we report on the implementation of an absorption technique that combines the advantages of frequency modulation spectroscopy for noise reduction and cavity-enhanced spectroscopy for increasing the interaction length between the light beam and the sample. This extremely sensitive technique, known as noise-immune cavity-enhanced optical heterodyne molecular spectroscopy (NICE-OHMS) [22–25], was applied to molecular frequency standards [26] and to precision measurements on molecules of astrophysical interest [27]. In the present study, weak electric dipole transitions in HD have been saturated, allowing for a reduction in line-width, that is almost four orders of magnitude narrower than the Doppler-broadened lines previously reported [19]. The experimental scheme is depicted in Fig. 1, where the spectroscopy laser is simultaneously locked to the stable optical cavity, and also to a Cs-clock-referenced frequency comb laser to provide an absolute frequency scale during the measurements.

The 48.2 cm long high-finesse (finesse $\sim 130\,000$) cavity comprises a pair of curved high-reflectors (Layertec, 1 m radius of curvature), with one of the mirrors mounted on a piezoelectric actuator. This stabilized optical cavity also provides short-term frequency stability to the spectroscopy laser, and transfers the absolute accuracy of the frequency standard. The setup provides an intracavity power in the order of 100 W that is sufficient for saturating HD transitions, while the equivalent absorption path length amounts to ~ 40 km. The cavity itself is enclosed within a vacuum chamber, which can be pumped and filled with the

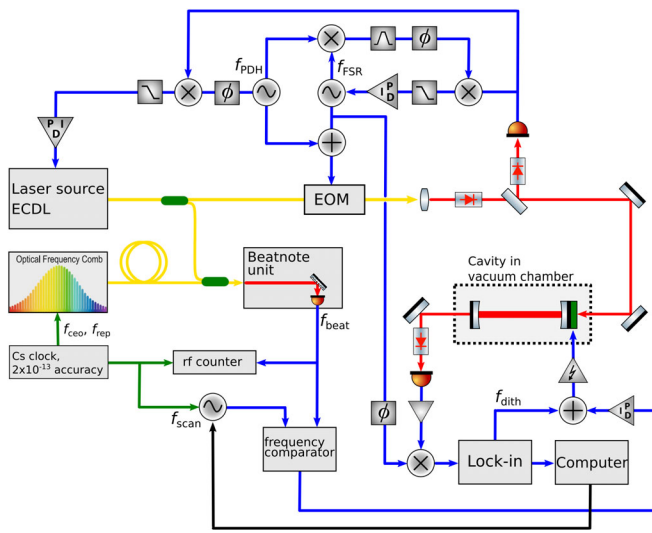


FIG. 1. Experimental setup. The spectroscopy laser (ECDL) is sent through a modulator (EOM) to impose both f_{PDH} and f_{FSR} modulations. f_{PDH} is used to stabilize the laser (carrier) frequency to the optical cavity (also the HD absorption cell) and f_{FSR} to generate sideband frequencies that are resonant to adjacent cavity modes. The spectroscopy laser is locked to a Cs atomic clock via an optical frequency comb laser for long-term stabilization. Additional cavity-length dither modulation f_{dith} is applied for lock-in detection of the HD saturated absorption signals.

HD gas sample, that is inserted through a liquid-nitrogen cooled trap for purification.

The laser source [an external-cavity diode laser (ECDL), Toptica DL Pro] operating at around $1.38 \mu\text{m}$ is mode matched and phase locked to the optical cavity. The laser beam is fiber coupled and split, with one part for the frequency calibration and metrology, while the main part is phase-modulated through a fiber-coupled electro-optic modulator (EOM) (Jenoptik PM1310), allowing for the simultaneous modulation of two frequencies $f_{\text{PDH}} \sim 20 \text{ MHz}$ and $f_{\text{FSR}} \sim 310 \text{ MHz}$. The beam reflected from the cavity is collected onto an amplified photoreceiver, the signal of which is divided for locking both the laser frequency f_{opt} via the Pound-Drever-Hall (PDH) scheme [28] and the cavity free spectral range frequency f_{FSR} with the DeVoe-Brewer scheme [29]. The beam transmitted through the cavity is collected with another high-speed photoreceiver, with the amplified signal demodulated at f_{FSR} in a double-balanced mixer. The resulting dispersive NICE-OHMS signal is sent to a lock-in amplifier to extract the $1f$ signal component at the dither frequency $f_{\text{dith}} \sim 430 \text{ Hz}$ with a peak-to-peak amplitude of 80 kHz . The noise equivalent absorption for the setup is estimated to be $1 \times 10^{-12}/(\text{cm}\sqrt{\text{Hz}})$.

The long term frequency stability and accuracy of the system is obtained by beating the spectroscopy laser with a frequency comb (Menlo Systems FC1500-250-WG) stabilized to a Cs clock frequency standard (Microsemi CSIII Model 4301B). The acquired beat note frequency f_{beat} is

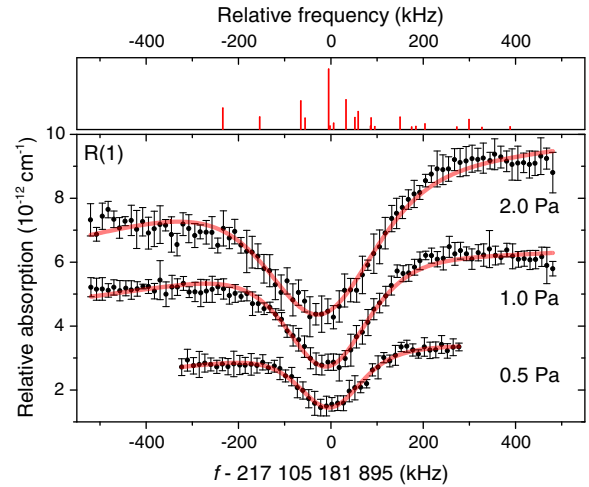


FIG. 2. Recordings of the HD (2,0) $R(1)$ line for three different pressure conditions averaging 5 scans for 2.0 Pa, 7 scans for 1.0 Pa, and 4 scans for 0.5 Pa. The solid (red) lines are fits using a line shape function based on a derivative of dispersion [23] while allowing for a baseline slope. The curves have been shifted in the vertical direction for clarity. In the upper panel a stick spectrum of the hyperfine structure of this transition is plotted, where the 0-value represents the center-of-gravity.

measured by an rf counter, and it is used to generate the steering signal for locking the cavity length, thereby tuning the laser frequency f_{opt} , which is determined via

$$f_{\text{opt}} = f_{\text{ceo}} + n \times f_{\text{rep}} + f_{\text{beat}}, \quad (1)$$

where $f_{\text{ceo}} = 20 \text{ MHz}$ is the carrier-envelope frequency offset of the frequency comb laser, $f_{\text{rep}} \sim 250 \text{ MHz}$ is its repetition rate, and $n \sim 8.7 \times 10^5$ is the mode number. The absolute frequency of f_{opt} is determined with an accuracy better than 1 kHz .

The $R(1)$ transition was recorded at different pressures (see Fig. 2), where each curve is an average of 4 to 7 scans. A typical scan takes about 12 minutes, with frequency intervals of 12.5 kHz , and with each data point averaged over 6 seconds. Figure 3 displays weaker resonances,

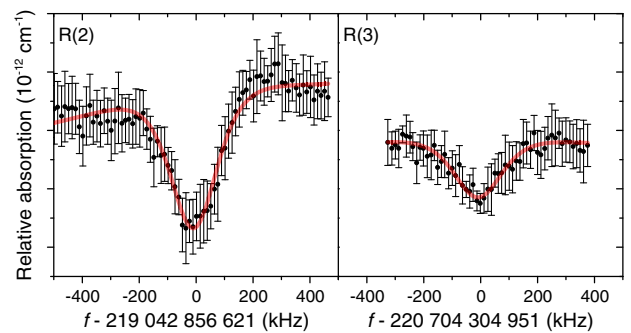


FIG. 3. The saturation spectra of the $R(2)$ and $R(3)$ transitions of the HD (2,0) overtone band at 1 Pa pressure. [$R(2)$: 12-scan average; $R(3)$: 5-scan average]

where the $R(2)$ spectrum is an average of 12 scans and that of $R(3)$ an average of 5 scans.

The assessment of systematic effects was performed primarily on the $R(1)$ transition, where the signal-to-noise ratio is the highest. The $R(1)$ transition frequency was measured at different pressures in the range 0.5–5.0 Pa (some shown in Fig. 2) displaying widths in the range 150–400 kHz [see Fig. 4(b)]. This allowed the determination of a pressure-dependent shift coefficient at $-9(3)$ kHz/Pa [see Fig. 4(a)] and for extrapolation to a zero-pressure transition frequency for $R(1)$. This collisional shift coefficient is an order-of-magnitude larger (but with similar sign), compared with coefficients for H_2 , obtained from studies (e.g., [10]) involving pressures higher than kPa. For $R(2)$ and $R(3)$ transitions measured at 1 Pa, a pressure shift correction of -9 kHz was applied. This seems appropriate in view of the study on H_2 [11] and D_2 [13], where it was shown that the collisional shift parameters depend only slightly on the rotational quantum number.

As seen in Fig. 2, there is an increase in line shape asymmetry with increasing pressure to which several effects, associated with line broadening can contribute. This asymmetry ultimately limits the present determination of the transition center to an accuracy of $\sim 1/5$ of the observed resonance width. We adopt a phenomenological approach to assess line shape profiles by Gaussian and Lorentzian functions, and a function based on a derivative of dispersion [23] (plotted in Figs. 2 and 3), as well as linear baseline fits. The baseline variation from scan-to-scan can be attributed to residual amplitude modulation. For the $R(1)$ line, all fits converge to a transition center within 15 kHz from each other, while a convergence to 20 kHz is found for the weaker transitions.

Saturation spectroscopy in a cavity leads to a photon recoil doublet that is symmetric to the recoil-free transition

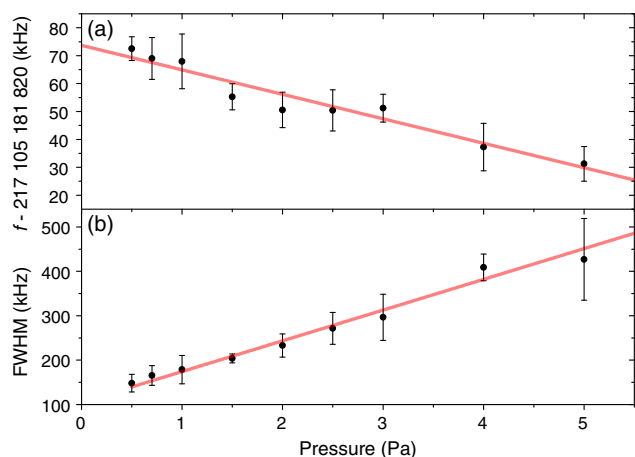


FIG. 4. A pressure-dependent frequency shift (a) and broadening (b) of the $R(1)$ transition in the 0.5 to 5 Pa pressure range. Note that for the broadening, the apparent width is plotted, measured via $1f$ -modulation of the NICE-OHMS signal (see text).

center [30]. For the HD (2,0) transitions at $1.38 \mu\text{m}$, the recoil shift is 34 kHz, resulting in a doublet splitting of 68 kHz but not producing a systematic shift. At half the intracavity laser power, no significant shift of the line center is observed, and we estimate an upper limit of 10 kHz for the power-dependent or AC-Stark shift. The second-order Doppler shift is calculated to be 1 kHz for a most probably velocity of 700 m/s (see below).

The collisional or pressure broadening, plotted in Fig. 4(b) for the $R(1)$ line, follows a linear behavior with a slope of $70(7)$ kHz/Pa. It is remarkable that the linear trend extends even to the lowest pressure of 0.5 Pa, at which the width is 150 kHz (FWHM). The linewidth of 150 kHz and the values presented in Fig. 4(b) correspond to widths that are artificially narrowed by the 430 Hz frequency modulation and the associated detection of the $1f$ derivative on the lock-in detector. Modeling of this phenomenon confirms that the recorded width of 150 kHz translates to a true FWHM linewidth of around 300 kHz for the absorption feature. The recoil doublet splitting of 68 kHz, a Rabi frequency of 20 kHz for the different transitions at peak intensity [31,32], and the hyperfine substructure must contribute to this linewidth. The latter also contributes to the asymmetry (see Fig. 2 and text below). An absorption width of 300 kHz is more than three times less than the transit-time rate (FWHM) of 1.3 MHz for HD molecules at room temperature and for the laser beam waist of $450 \mu\text{m}$ [31,32]. Similar observations of strongly reduced linewidths below the transit-time rate have been shown in methane [33,34] and acetylene [23], where it was attributed to the dominant contribution of slow-moving molecules in the saturation signal. Even if the entire width of 300 kHz is attributed to transit-time broadening, this would correspond to a most probable speed of 720 m/s. However, in view of the other linewidth contributions discussed above, the most probable velocity may be even lower.

The hyperfine structure of the $v = 0$ levels in HD was investigated by Ramsey and co-workers using molecular beam resonance techniques [35,36]. *Ab initio* calculations of hyperfine constants for $v = 2$ and $v = 0$ levels in HD [37], at most differing at 6.5% between vibrational levels, are found to be in good agreement with experiment for $v = 0$ [35]. Based on this, the hyperfine substructure of the $R(1)$ transition, composed of 21 components, was calculated and represented by a stick spectrum plotted in the upper panel of Fig. 2. While the entire hyperfine structure covers a range of 500 kHz, the three most intense hyperfine components fall within a span of 100 kHz around the center-of-gravity, demonstrating that the observed effective linewidth of 300 kHz is compatible with the hyperfine substructure. From this clustering of strongest components around the zero position (see Fig. 2), we conclude that the hyperfine structure does not significantly shift the center frequency of the transition. However, some asymmetry of the line shape, and possibly the background slope, might be due to the unresolved hyperfine structure [38].

TABLE I. List of corrections Δf and uncertainty estimates σ_f in units of kHz for the transition frequencies.

Contribution	$R(1)$		$R(2), R(3)$	
	Δf	σ_f	Δf	σ_f
Line fitting	0	15	0	20
Pressure shift ^a	0	3	-9	6
2nd-order Doppler	1	1	1	1
AC-Stark shift	0	10	0	10
Frequency calibration	0	<1	0	<1
Subtotal systematic	1	19	-8	23
Statistics	0	10	0	15
Total	1	20	-8	28

^a $R(1)$ has been extrapolated to zero pressure, while for $R(2)$ and $R(3)$, a correction is applied based on pressure-shift coefficient of $R(1)$.

Table I lists the error budget of the present study. The statistics entry demonstrates the reproducibility of measurements performed on different days, in some cases after realignment, with the best statistics at 10 kHz obtained for $R(1)$. We estimate a total uncertainty, including systematics, of $\sigma_f = 20$ kHz for the $R(1)$ transition frequency and $\sigma_f = 28$ kHz for the $R(2)$ and $R(3)$ resonances. Resulting transition frequencies of the $R(1)$, $R(2)$, and $R(3)$ lines are listed in Table II. These values are compared to results of the previous experimental determination by Kassi and Campargue [19], obtained under Doppler-broadened conditions, showing good agreement, with the present results representing a three order of magnitude improvement in accuracy. Theoretical level energy calculations by Pachucki and Komasa [21] were claimed to be accurate to 30 MHz, but values were provided to 3 MHz (10^{-4} cm⁻¹) accuracy. Since we compare with the energy splittings between $v = 0$ and $v = 2$, the theoretical transition frequencies in Table II should be more accurate because of cancellations in various energy contributions. This assessment of the calculation uncertainty is supported by the excellent agreement between our measurements and the theoretical values that are better than 2 MHz.

The 30 kHz absolute accuracy (10^{-10} relative accuracy) achieved in this study constitutes a 1000-fold improvement over previous work, and it demonstrates the first sub-Doppler determination of pure ground state transitions in

HD and, in fact, in any molecular hydrogen isotopologue. The experimental results challenge current investigations in first principles relativistic theory and QED calculations of the benchmark hydrogen molecules [2,3,21,39]. When such calculations reach the same accuracy level as the experiment, there is a potential to constrain theories of physics beyond the Standard Model, as was shown previously [7,8]. The finite size of the proton contributes ~ 300 kHz to the H₂ (3,0) overtone transition [40], and a similar contribution is expected for the HD transitions investigated here. If theory and experiment reach the kHz accuracy level, this will allow for a determination of the proton size to 1% accuracy. Along with complementary investigations in the electronic [41] and muonic hydrogen atoms [42], neutral and ionic molecular hydrogen [43], the HD overtone determinations may contribute towards the resolution of the conundrum known as the proton-size puzzle.

The authors wish to thank Prof. J. Gauss (Mainz) for a calculation of hyperfine constants in HD $v = 0$ and $v = 2$ levels. P.D. is supported by the CNRS. W.U. acknowledges the European Research Council for an ERC-Advanced Grant under the European Union's Horizon 2020 research and innovation programme (Grant agreement No. 670168).

Note added in proof.—Recently, we were informed about the outcome of a measurement of the HD $R(1)$ line by Lamb-dip cavity ring down spectroscopy by the Hefei group [44], deviating by 900 kHz from our result. In an attempt to find the origin of this discrepancy, both groups measured a stronger $R(4)$ line in C₂H₂, yielding 217043458139 (6) kHz at Amsterdam and 217043458146 (8) kHz at Hefei. This agreement demonstrates that the discrepancy is not due to differences between spectroscopic techniques, nor in metrology issues like locking of lasers or beat-note measurements. In our laboratory, we found no difference when the C₂H₂ line was measured with and without the option of low-frequency modulation and lock-in detection, thus demonstrating that this mode of operation has no effect on the line center frequency. In addition, the measurement of the HD $R(1)$ transition, with linear and with circular polarization in the cavity, resulted in the same transition frequency, proving that optical pumping does not play a role.

 TABLE II. A comparison of R -branch transition frequencies in the HD (2,0) band obtained from the present study with previous experimental determination Δ_{exp} [19], and with most accurate *ab initio* calculations Δ_{calc} [21]. Values are given in MHz with uncertainties in units of the last digit indicated in between parentheses. See text for a discussion of the theoretical uncertainty.

Line	This study	Ref. [19]	Δ_{exp}	Theory [21]	Δ_{calc}
$R(1)$	217105181.895(20)	217105192(30)	-10	217105180	2
$R(2)$	219042856.621(28)	219042877(30)	-20	219042856	1
$R(3)$	220704304.951(28)	220704321(30)	-16	220704303	2

- [1] K. Piszczatowski, G. Łach, M. Przybytek, J. Komasa, K. Pachucki, and B. Jeziorski, *J. Chem. Theory Comput.* **5**, 3039 (2009).
- [2] K. Pachucki and J. Komasa, *J. Chem. Phys.* **144**, 164306 (2016).
- [3] M. Puchalski, J. Komasa, P. Czachorowski, and K. Pachucki, *Phys. Rev. Lett.* **117**, 263002 (2016).
- [4] J. Liu, E. J. Salumbides, U. Hollenstein, J. C. J. Koelemeij, K. S. E. Eikema, W. Ubachs, and F. Merkt, *J. Chem. Phys.* **130**, 174306 (2009).
- [5] D. Sprecher, C. Jungen, W. Ubachs, and F. Merkt, *Faraday Discuss. Chem. Soc.* **150**, 51 (2011).
- [6] G. D. Dickenson, M. L. Niu, E. J. Salumbides, J. Komasa, K. S. E. Eikema, K. Pachucki, and W. Ubachs, *Phys. Rev. Lett.* **110**, 193601 (2013).
- [7] E. J. Salumbides, J. C. J. Koelemeij, J. Komasa, K. Pachucki, K. S. E. Eikema, and W. Ubachs, *Phys. Rev. D* **87**, 112008 (2013).
- [8] E. J. Salumbides, A. N. Schellekens, B. Gato-Rivera, and W. Ubachs, *New J. Phys.* **17**, 033015 (2015).
- [9] S. Kassı and A. Campargue, *J. Mol. Spectrosc.* **300**, 55 (2014).
- [10] C.-F. Cheng, Y. R. Sun, H. Pan, J. Wang, A.-W. Liu, A. Campargue, and S.-M. Hu, *Phys. Rev. A* **85**, 024501 (2012).
- [11] Y. Tan, J. Wang, C.-F. Cheng, X.-Q. Zhao, A.-W. Liu, and S.-M. Hu, *J. Mol. Spectrosc.* **300**, 60 (2014).
- [12] P. Maddaloni, P. Malara, E. De Tommasi, M. De Rosa, I. Ricciardi, G. Gagliardi, F. Tamassia, G. Di Lonardo, and P. De Natale, *J. Chem. Phys.* **133**, 154317 (2010).
- [13] S. Kassı, A. Campargue, K. Pachucki, and J. Komasa, *J. Chem. Phys.* **136**, 184309 (2012).
- [14] D. Mondelain, S. Kassı, T. Sala, D. Romanini, D. Gatti, and A. Campargue, *J. Mol. Spectrosc.* **326**, 5 (2016).
- [15] S. Bubin, F. Leonarski, M. Stanke, and L. Adamowicz, *J. Chem. Phys.* **130**, 124120 (2009).
- [16] G. Herzberg, *Nature (London)* **166**, 563 (1950).
- [17] K. Pachucki and J. Komasa, *Phys. Rev. A* **78**, 052503 (2008).
- [18] A. R. W. McKellar, *Can. J. Phys.* **51**, 389 (1973).
- [19] S. Kassı and A. Campargue, *J. Mol. Spectrosc.* **267**, 36 (2011).
- [20] P. Wcisłó, I. E. Gordon, C.-F. Cheng, S.-M. Hu, and R. Ciuryłó, *Phys. Rev. A* **93**, 022501 (2016).
- [21] K. Pachucki and J. Komasa, *Phys. Chem. Chem. Phys.* **12**, 9188 (2010).
- [22] J. Ye, L.-S. Ma, and J. Hall, *Opt. Lett.* **21**, 1000 (1996).
- [23] L.-S. Ma, J. Ye, P. Dubé, and J. Hall, *J. Opt. Soc. Am. B* **16**, 2255 (1999).
- [24] F. Schmidt, A. Foltynowicz, W. Ma, T. Lock, and O. Axner, *Appl. Phys. B* **101**, 497 (2010).
- [25] A. Foltynowicz, I. Silander, and O. Axner, *J. Opt. Soc. Am. B* **28**, 2797 (2011).
- [26] H. Dinesan, E. Fasci, A. d'Addio, A. Castrillo, and L. Gianfrani, *Opt. Express* **23**, 1757 (2015).
- [27] C. Markus, J. Hodges, A. Perry, G. Kocheril, H. Müller, and B. McCall, *Astrophys. J.* **817**, 138 (2016).
- [28] R. W. P. Drever, J. L. Hall, F. V. Kowalski, J. Hough, G. M. Ford, A. J. Munley, and H. Ward, *Appl. Phys. B* **31**, 97 (1983).
- [29] R. G. DeVoe and R. G. Brewer, *Phys. Rev. A* **30**, 2827 (1984).
- [30] J. L. Hall, C. J. Bordé, and K. Uehara, *Phys. Rev. Lett.* **37**, 1339 (1976).
- [31] P. Dupré, *J. Opt. Soc. Am. B* **32**, 838 (2015).
- [32] P. Dupré, *J. Quant. Spectrosc. Radiat. Transfer* **205**, 196 (2018).
- [33] S. N. Bagaev, L. S. Vasilenko, A. K. Dmitriev, M. N. Skvortsov, and V. P. Chebotaev, *JETP Lett.* **23**, 360 (1976).
- [34] S. N. Bagaev, A. E. Baklanov, A. S. Dychkov, P. V. Pokasov, and V. P. Chebotaev, *JETP Lett.* **45**, 471 (1987).
- [35] N. F. Ramsey and H. R. Lewis, *Phys. Rev.* **108**, 1246 (1957).
- [36] R. F. Code and N. F. Ramsey, *Phys. Rev. A* **4**, 1945 (1971).
- [37] J. Gauss (private communication).
- [38] G. Giusfredi, S. Bartalini, S. Borri, P. Cancio, I. Galli, D. Mazzotti, and P. De Natale, *Phys. Rev. Lett.* **104**, 110801 (2010).
- [39] K. Pachucki and J. Komasa, *J. Chem. Phys.* **141**, 224103 (2014).
- [40] M. Puchalski, J. Komasa, and K. Pachucki, *Phys. Rev. A* **95**, 052506 (2017).
- [41] A. Beyer, L. Maisenbacher, A. Matveev, R. Pohl, K. Khabarova, A. Grinin, T. Lamour, D. C. Yost, T. W. Hänsch, N. Kolachevsky *et al.*, *Science* **358**, 79 (2017).
- [42] R. Pohl, A. Antognini, F. Nez, F. D. Amaro, F. Biraben, J. M. R. Cardoso, D. S. Covita, A. Dax, S. Dhawan, L. M. P. Fernandes *et al.*, *Nature (London)* **466**, 213 (2010).
- [43] J. Biesheuvel, J.-P. Karr, L. Hilico, K. S. E. Eikema, W. Ubachs, and J. C. J. Koelemeij, *Nat. Commun.* **7**, 10385 (2016).
- [44] L.-G. Tao, A.-W. Liu, K. Pachucki, J. Komasa, Y. R. Sun, J. Wang, and S.-M. Hu, preceding Letter, *Phys. Rev. Lett.* **120**, 153001 (2018).